Accepted Manuscript online: 2023-01-04 Article published online: 2023-02-27

Common Key Genes in Differentiating Parathyroid Adenoma From Thyroid Adenoma

OPEN ACCESS

Authors
Yanbin Lin[1, 2], Jinxuan He[1], Zhixiang Mou[1], Yuchen Tian[1, 2], Huiting Chen[1], Tianjun Guan[1], Lan Chen[1]

Affiliations
1 Department of Nephrology, Zhongshan Hospital Xiamen University, Xiamen, China
2 School of Medicine, Xiamen University, Xiamen, China

Key words
parathyroid adenoma, thyroid adenoma, thyroid, key genes, bioinformatics, drug prediction

received 23.10.2022
accepted after revision 15.12.2022
accepted manuscript online 04.01.2023

Bibliography
Horm Metab Res 2023; 55: 212–221
DOI 10.1055/a-2007-2631
ISSN 0018-5043

Georg Thieme Verlag KG, Rüdigerstraße 14,
70469 Stuttgart, Germany

Correspondence
Lan Chen
Zhongshan Hospital Xiamen University
Department of Nephrology
Xiamen Municipal Health Commission, Building B, Tianlu Building, 2 Tong ‘an Road, Xiamen city
361003 Fujian Province
China
Tel.: 15060120551
chenlan@xmu.edu.cn

ABSTRACT

Recent studies have demonstrated the close relationship between parathyroid adenoma (PA) and thyroid follicular adenoma (FTA). However, the underlying pathogenesis remains unknown. This study focused on exploring common pathogenic genes, as well as the pathogenesis of these two diseases, through bioinformatics methods. This work obtained PA and FTA datasets from the Integrated Gene Expression Database to identify the common differentially expressed genes (DEGs) of two diseases. The functions of the genes were investigated by GO and KEGG enrichment. The program CytoHubba was used to select the hub genes, while receiver operating characteristic curves were plotted to evaluate the predictive significance of the hub genes. The DGIbd database was used to identify gene-targeted drugs. This work detected a total of 77 DEGs. Enrichment analysis demonstrated that DEGs had activities of 3′,5′-cyclic AMP, and nucleotide phosphodiesterases and were associated with cell proliferation. NOS1, VWF, TGFBR2, CAV1, and MAPK1 were identified as hub genes after verification. The area under the curve of PA and FTA was > 0.7, and the hub genes participated in the Relaxin Signaling Pathway, focal adhesion, and other pathways. The construction of the mRNA-miRNA interaction network yielded 11 important miRNAs, while gene-targeting drug prediction identified four targeted drugs with possible effects. This bioinformatics study demonstrated that cell proliferation and tumor suppression and the hub genes co-occurring in PA and FTA, have important effects on the occurrence and progression of two diseases, which make them potential diagnostic biomarkers and therapeutic targets.

Introduction

Parathyroid adenoma (PA) is a common factor leading to primary hyperparathyroidism and has been considered to be the result of the clonal expansion of tumor cells [1, 2]. Current research on parathyroid disease has significantly improved our understanding of parathyroid adenomas, which manifest in a variety of clinicopathological entities. Pathologists evaluating PA find it difficult to distinguish between parathyroid cancer and atypical parathyroid adenoma. Recent studies have also reported that the size of parathyroid adenoma is associated with calcium or parathyroid hormone levels accompanied by genetic mutations [3]. However, the pathogenesis of the size and genetic changes of parathyroid adenoma remains unclear.

Thyroid dysfunction and increased parathyroid hormone and germline mutation inactivation of oncogene suppressor are all common causes of parathyroid adenoma. It has been found that parathyroid and thyroid glands share homology in the embryonic stage, adjacency after maturation, and some similarities in the process of cell proliferation and development. Therefore, it is necessary to further study the relationship between the two disease states [4–7]. The glycosphingolipid patterns of human parathyroid glands and thyroid glands are very similar, according to studies, and GD1a is expressed on the cell surface of parathyroid glands and in the cytoplasm of thyroid glands [8]. According to the Classification Overview of Parathyroid Tumors released by the World Health Organization in 2022, a parathyroid adenoma is histologically a well-defined tumor in which follicular structures often form, which can be mistaken for follicular thyroid adenoma (FTA), if prominent [9]. In a retrospective study of PA patients complicated with thyroid disease, it was found that blood PTH level was negatively correlated with the TT4 and FT4 levels, suggesting that hyperparathyroidism plays an inhibitory role in thyroid adenoma function [10]. Walker et al. discovered that in rats with hypothyroidism, continuous TSH stimulation caused neoplastic lesions in the parathyroid glands, resulting in hyperparathyroidism [11]. These findings suggest that PA and FTA may have common pathogenesis. The search for new biomarkers to predict the coexistence of these two diseases is critical, as needle biopsy is an invasive procedure with some bleeding risk and inaccuracy.

Bioinformatics techniques have been widely used to analyze microarray data in recent years, and microarray technology combined with web-based analysis can provide valuable information about gene expression signatures in various cancers. The authors of a study on epigenetic changes in PAs used bioinformatics to demonstrate for the first time the difference in circRNA expression pattern between sporadic parathyroid adenomas and normal parathyroid tissues, as well as the effect of gender on the epigenetic regulation of PA [12]. Other studies have found that miRNAs like miR-222 [13], miR-503 [13], and miR-517c [14] are significantly upregulated in parathyroid carcinoma. Bioinformatics has also been used to identify key genes and molecular pathways in parathyroid neoplasms [15], and thyroid cancer microarray profiles have been examined to investigate differential gene expression and pathway enrichment [16]. Ameri et al. successfully used bioinformatics methods to screen biomarkers for follicular thyroid carcinoma (FTC) and FTA. Although research into PA and FTA continues, there has been no study to show a common biomarker of the two diseases, and the interaction and prognosis of the two diseases remain unknown. Therefore, we focused on the biomarker research of PA and FTA. We used the comprehensive database from gene expression microarray data, tried to use bioinformatics analysis to explore the potential pathogenic genes and diagnostic biomarkers common to PA and FTA, and assessed drugs against the target genes to predict the results. Further research for clinical diagnosis and treatment is essential to provide new drug targets to cure disease.

Materials and Methods

Data sources

We searched for the gene expression profiles of patients with PA and FTA in the Gene Expression Database (GEO) (https://www.ncbi.nlm.nih.gov/geo/) using the terms "parathyroid adenoma" or "follicular thyroid adenoma". The obtained datasets were screened based on the following criteria: first, the profile must cover cases and controls. Second, each sample must be of human origin. Third, the data type is total RNA. Finally, these datasets should provide original information for subsequent analysis. We selected GSE83421 from GPL22020 (Human Operon V1.1 printed oligonucleotide array) and GSE54958 from GPL6244 (Affymetrix Human Gene 1.0 ST Array) for the next step.

Data analysis

First, we used the Linear Model of Microarray Data (LIMMA) package in the statistical software R to compare PA patients with normal controls, as well as FTA patients and their healthy controls, with filter criteria set at $|\log2FC| \geq 1$ and $p > 0.05$. We then used obtained intersection genes from the two sets of DEGs from the two disease groups using a Venn diagram.

Functional annotations for DEGs

To investigate the biological activities and signaling pathways affected by the common DEGs, we used the Gene Ontology (GO) enrichment analysis, which included biological processes (BPs), cellular components (CCs), and molecular functions (MFs) [17]. We also performed the Kyoto Encyclopedia of Genes and Genomes (KEGG) analysis [18]. The screened DEGs were input in the web-based tool Database for Annotation, Visualization, and Integrated Discovery (DAVID) (https://david.ncifcrf.gov/), for the GO and KEGG analysis with $p < 0.05$. The protein-protein interaction (PPI) network analysis and identification of hub genes were performed using DEGs based on the STRING database (https://string-db.org/) [19], and the software Cytoscape (version 3.9.0) was used to import the obtained data [20]. Seven topological analysis methods (MCC, MNC, EPC, Degree, Closeness, Radiality, and Stress) were used in the CytoHubba plug-in. The degree, closeness, radiality, stress, and EPC for the first 10 core genes were determined to finally obtain five co-expressed key core genes by obtaining intersection through UpsetR.

Construction and validation of the co-expression network of key core genes

Then, through the GeneMANIA database (http://www.genemania.org/), we built the hub genes expression network, which identified

the gene set internal reliable tools using the pROC and ggplot2 (R3.6.3). Receiver operating characteristic (ROC) curves were plotted to analyze whether our selected target genes were sensitive and specific. Then, the area under the ROC curve (AUC) was used to quantify the results. An AUC value greater than 0.6 was considered diagnostic.

Construction of the mRNA-miRNA regulatory network

The online database NetworkAnalyst version 3.0 (https://www.mirnet.ca/) was used to predict associations between mRNAs and miRNAs [21]. Thereafter, we built an mRNA-miRNA regulatory network to describe the associations of miRNAs with mRNAs. The regulatory network was visualized using the Cytoscape software.

Establishment of gene-drug interaction

We used the DGIdb database (https://dgidb.org/) to obtain drug-gene interactions [22].

Results

Analysis of DEGs in PA and FTA

The GSE83421 and GSE54958 datasets were selected using the filtering conditions. The GSE83421 dataset contained 25 PA tissues and 6 healthy parathyroid tissues, while GSE54958 contained 7 FTA and 7 healthy thyroid tissues. GSE83421 had 687 DEGs identified by the LIMMA package, among which 607 DEGs were upregulated and 80 were downregulated. GSE54958 contained 8827 DEGs, including 3109 upregulated and 5730 downregulated DEGs. Using a Venn diagram, 77 common DEGs of the two diseases were obtained, as presented in ▶ **Table 1** and ▶ **Fig. 1 a–c**.

GO and KEGG Analysis

Then, GO, and KEGG analyses were performed on 77 common DEGs between PA and FTA. The results are presented in ▶ **Fig. 1d**. Regarding GO-BP terms, the DEGs were mainly enriched in response to estrogen, negative regulation of cellular response to growth factor stimulus, neurotransmitter reuptake, and negative regulation of the transmembrane receptor protein serine/threonine kinase pathway. Regarding the CC terms, DEGs were mostly associated with caveola, membrane microdomain, membrane raft, and plasma membrane raft. Regarding molecular function, the DEGs were associated with cyclic-nucleotide phosphodiesterase activity, 3′,5′-cyclic-nucleotide phosphodiesterase activity, cholesterol binding, and 3′,5′-cyclic-AMP phosphodiesterase activity. Unfortunately, KEGG enrichment analysis did not show the enrichment of DEGs in meaningful pathways.

▶ **Table 1** The 77 common DEGs of GSE83421 and GSE54958.

TCN1, SCN1A, ZNF304, IGKC, DLL4, MED6, TFAM, MID2, CLDN10, KPNA6, ELAC1, PDE3B, INPP5A, PCOLCE2, OR7E19P, MYO5C, FGF23, MT1B, CDC14B, IFNA8, RAE1, PNLIPRP1, SKIL, GDF3, HBP1, GRIN2A, NOS1, FBXO25, BFSP2, KLF1, MMP27, COX7A2, KCNJ10, PTRF, PAPOLB, MT1E, CLCA4, PDE7B, MAPK1, PDE6H, SPRY1, DGCR8, HEPH, TSKS, SDCCAG8, UTS2, AP1G1, APOA1, APBB2, LXN, VWF, LDB2, CLIC4, PITX2, LRP8, OGN, RPS6KA3, PRRG1, PER2, CD24, GIT1, SMURF2, BPESC1, STX7, RGS13, SYT13, CAV1, SBF1. YWHAH, TGFBR2, MSN, HSPB1, APOD, TAGLN, CNN3, ADAMTS1, THBS4

Analysis based on PPI network and determination of hub genes

To determine the hub genes in the common DEGs of the two diseases, we built the PPI network (▶ **Fig. 2**). The interaction map of important proteins was obtained using the Cytoscape software, with a total of 36 nodes and 44 edges selected in MCC, MNC, EPC, Degree, Closeness, Radiality, and Stress. The top 10 genes of 7 topology algorithms in EPC, as well as 5 co-expressed genes (NOS1, VWF, TGFBR2, CAV1, and MAPK1), were obtained as hub genes by upset (▶ **Fig. 3**).

Assessment of the therapeutic effect and establishment of PPI network based on hub genes

The PPI network analysis on the five hub genes, along with the 20 intersected genes based on GeneMANIA, indicated that these genes showed a complex PPI network with a physical interaction rate of 77.64 %, co-expression rate of 8.01 %, prediction rate of 5.37 %, co-localization rate of 3.63 %, genetic interaction rate of 2.87 %, pathway rate of 1.88 %, and protein domain-sharing rate of 0.60 %. These estimated genes were within the outer circle, whereas the hub genes were within the inner circle. The network analysis demonstrated the enrichment of such genes into membrane microdomain, plasma membrane raft, membrane raft, coagulation, hemostasis, peptidyl-serine modification, and blood coagulation (▶ **Fig. 4**).

Similarly, the results of GO and KEGG analysis on five hub DEGs revealed the top 10 enriched GO categories, which are presented in ▶ **Fig. 5**. Regarding BP terms, the DEGs were mainly related to peptidyl-serine phosphorylation, peptidyl-serine modification, caveolin-mediated endocytosis, G protein-coupled receptor pathway related to heart processes, modulation of the heart contraction force, modulation of the negative potassium ion transport, blood coagulation, thymus development, regulation of MAP kinase activity, and hemostasis. Regarding CC terms, the DEGs were mainly related to membrane microdomain, membrane raft, plasma membrane raft, caveola, membrane region, sarcolemma, postsynaptic density, asymmetric synapse, secretory granule lumen, and cytoplasmic vesicular lumen. Regarding MF terms, the DEGs were mostly associated with ion channel binding, channel regulator activity, oxidoreductase activity, I-SMAD binding, heme proteins acceptor, action on NAD(P)H, activin binding, MAP kinase activity, nitric oxide synthase binding, transforming growth factor beta (TGFβ)-activated receptor activity, and FMN binding. In KEGG analysis, we focused on the common DEGs among the apelin pathway, focal adhesion, relaxin pathway, and long-term depression.

Then, ROC curves of the five hub gene levels were constructed to evaluate whether those genes could be used in diagnosis. The corresponding AUC for VWF, TGFBR2, CVA1, MAPK1, and NOS1 in PA patients and normal controls were 0.969, 0.954, 0.838, 0.769, and 0.731, respectively (▶ **Fig. 6**). The AUC for the hub genes in FTA patients and their controls were 1.00, 0.857, 1.00, 1.00, and 0.959, respectively. These results indicate that the AUC values of the five key genes in the two disease groups were > 0.7, while the VWF was

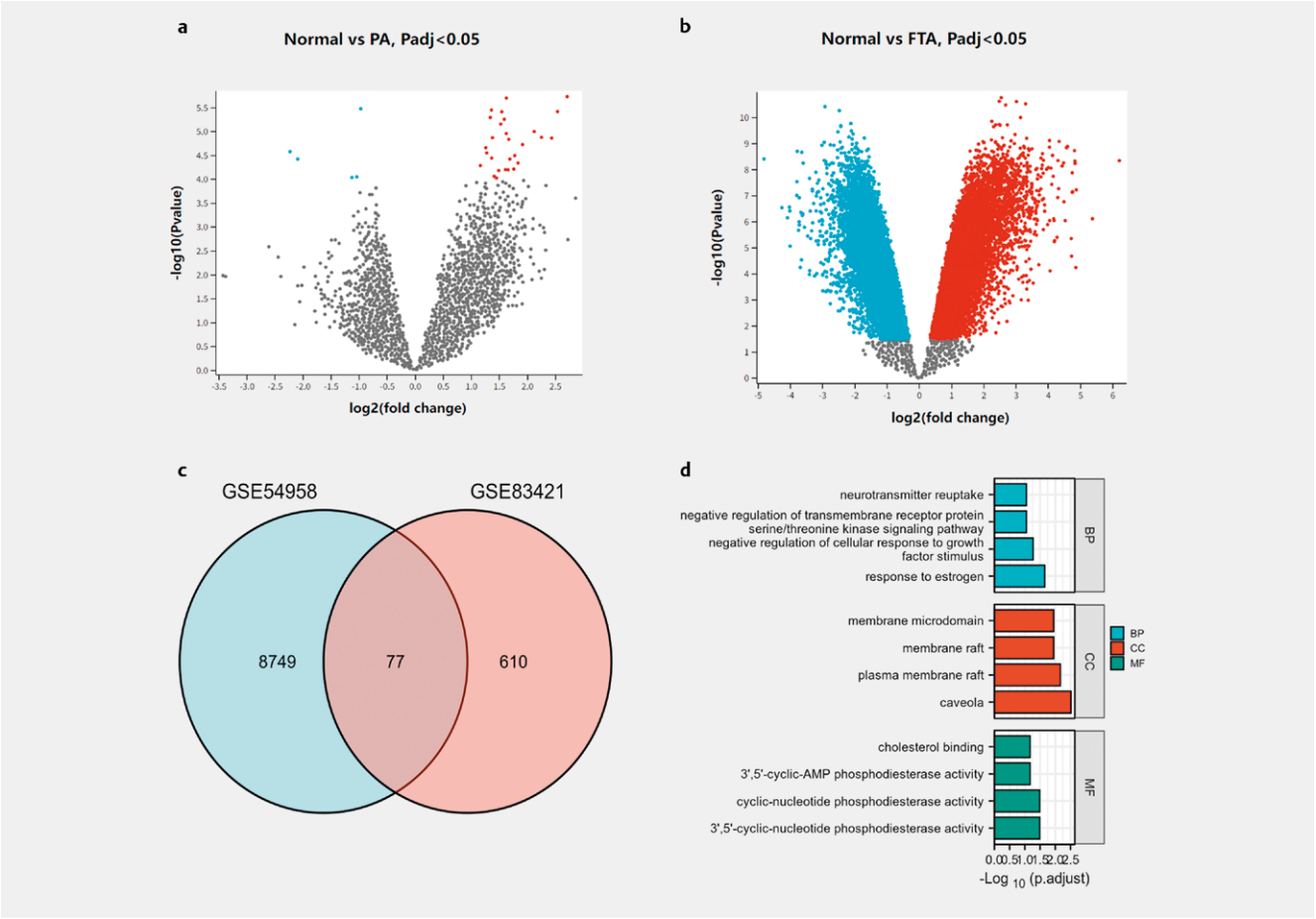

▶ **Fig. 1** Datasets analysis of GSE83421 and GSE54958. **a**,**b**: Volcano plot of the GSE83421 and GSE54958. Each point on the volcano map represents a gene. Blue indicates a downregulated gene, and red indicates an upregulation gene. **c**: Venn diagram of DEGs common to two GEO datasets. A total of 77 consistently expressed genes were identified from GSE83421 and GSE54958. **d**: KEGG and GO enrichment analyses of the 77DEGs. BP: Biological processes; CC: Cellular components; MF: Molecular function.

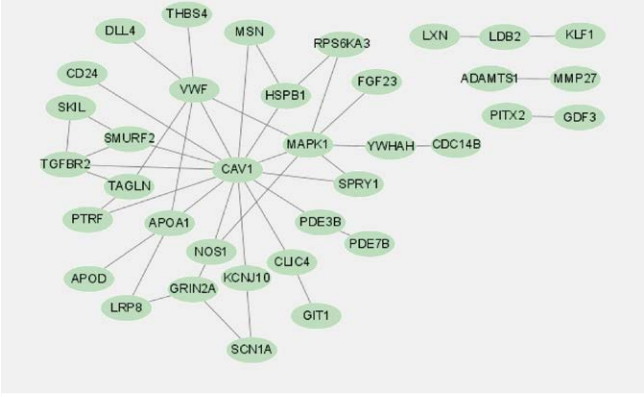

▶ **Fig. 2** PPI networks of DGEs.

> 0.9 in the two groups, suggesting that these hub genes were valuable in disease diagnosis.

Construction of mRNA – miRNA

We used the software NetworkAnalyst 3.0 to predict the target miRNAs of the key genes and eventually identified 310 target miRNAs for four hub genes, along with 370 pairs of mRNA-miRNAs and 183 miRNAs that regulated MAPK1. It was observed that 110 miRNAs regulated TGFBR2, 58 miRNAs regulated CAV1, and 19 miRNAs regulated NOS1. A total of 11 miRNAs were related to three key genes (▶ **Fig. 7**).

Establishment of gene-drug interactions

To analyze the gene-drug interactions, the five confirmed hub genes were imported into the DGIdb database. The genes VWF, TGFBR2, MAPK1, and NOS1 were identified and blended with four predicted therapeutic agents (Caplacizumab, Ravoxertinib, Ketamine, Fostamatinib) (▶ **Table 2**). We identified Caplacizumab as a targeted drug of VWF, with an interaction fraction of 13.25. As VWF was an important differential gene in the two diseases, Caplacizumab may be a potential therapeutic agent.

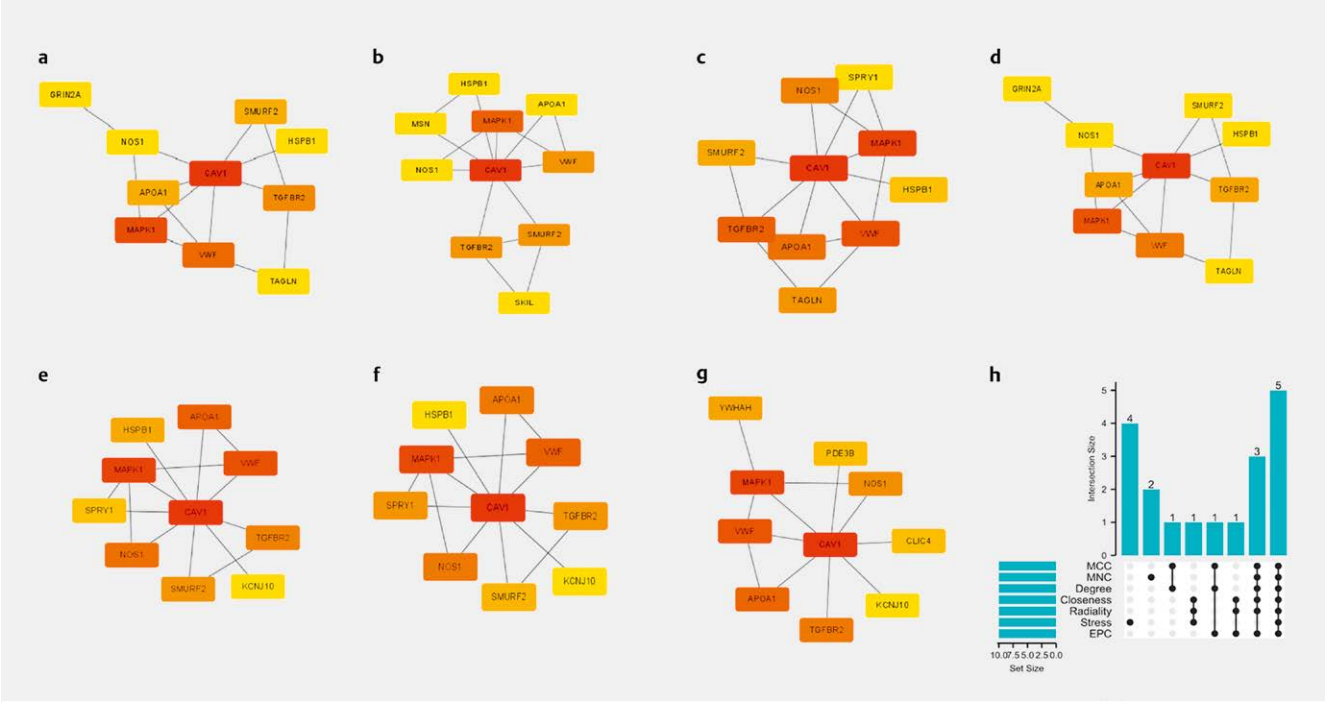

▶ **Fig. 3** Top10 DEGs in the PPI works by seven topological analysis methods. The Venn diagram shows five co-expressed key core genes by obtaining intersection through UpsetR.

Discussion

Although PA and FTA have similar pathology and adjacent location, their pathogenesis remains unclear. This study adopted bioinformatics analysis to obtain the important co-expressing DEGs between PA and FTA (NOS1, VWF, TGFBR2 CAV1, and MAPK1), and the roles of these DEGs in cell proliferation and tumor suppression were assessed by enrichment analysis.

We screened two datasets from the GEO database using the R language and identified 77 co-expressed DEGs. Among them, 40 genes showed the same expression trend in the two diseases, including 30 upregulated genes and 10 downregulated genes. According to the GO and KEGG pathway analysis of DEGs, they had 3′,5′-cyclic nucleotide or AMP phosphodiesterase activities and were associated with cell proliferation. After the construction of the PPI interaction network using the Cytoscape plug-in in seven different algorithms, we selected five important hub genes (NOS1, VWF, TGFBR2 CAV1, and MAPK1). According to the GO enrichment analysis, hub genes were primarily involved in plasma membrane raft, membrane microdomain, coagulation, and hemostasis, indicating that the key genes were involved in cell membrane construction and hemostasis activities. This demonstrates that the presence of PA and FTA is accompanied by obvious cell proliferation, and blood supply and hemostasis are critical links in the proliferation process. Based on the KEGG pathway analysis, the hub genes participated in the relaxin pathway, relaxin signaling pathway, and focal adhesion pathway. The Relaxin signaling pathway is activated during disease development, which transmits cAMP signaling and regulates the process of gene transcription to inhibit fibrosis. Cell proliferation and tumor growth can be induced in the apelin signaling pathway. Focal adhesion is closely related to tumor adhesion and is highly expressed in various cancer cells, which promotes the growth, survival, proliferation, adhesion, metastasis, and angiogenesis of cancer cells. In this study, the above three pathways were enriched, indicating that adenomatosis is correlated with gene regulation and cell proliferation in cancer, although the specific mechanism needs further investigation. In the diagnostic ROC analysis, the five hub genes had strong diagnostic values, and 11 important miRNAs were obtained in the construction of the mRNA-miRNA interaction network. These results indicate that the common DEGs of these two diseases are closely related to cell proliferation which further supports the current mainstream view.

NOS1-encoded proteins are members of the nitric oxide synthase family and act as mediators in a variety of biological processes. Following the stimulation of tumor necrosis factor and other related cytokines, the expression of the NOS1 gene can be upregulated, and the activity of antioxidant transcription factors can be increased, resulting in increased tumor tolerance to hypoxia and, eventually, tumor drug resistance [23]. Findings of an ovarian cancer drug-suppressor gene assay revealed that NOS1 could enhance the chemical resistance to DDP in ovarian cancer cells [24]. Furthermore, NOS1 inhibits mitochondrial reactive oxygen species and apoptosis in colon cancer cells [25]. At present, NOS1 has not been reported in the field of adenoma. According to the similarity between adenoma and adenocarcinoma, and the expression level of NOS1 in the two diseases is higher than that in the normal group in this study, indicating that NOS1 may play an important role in adenoma.

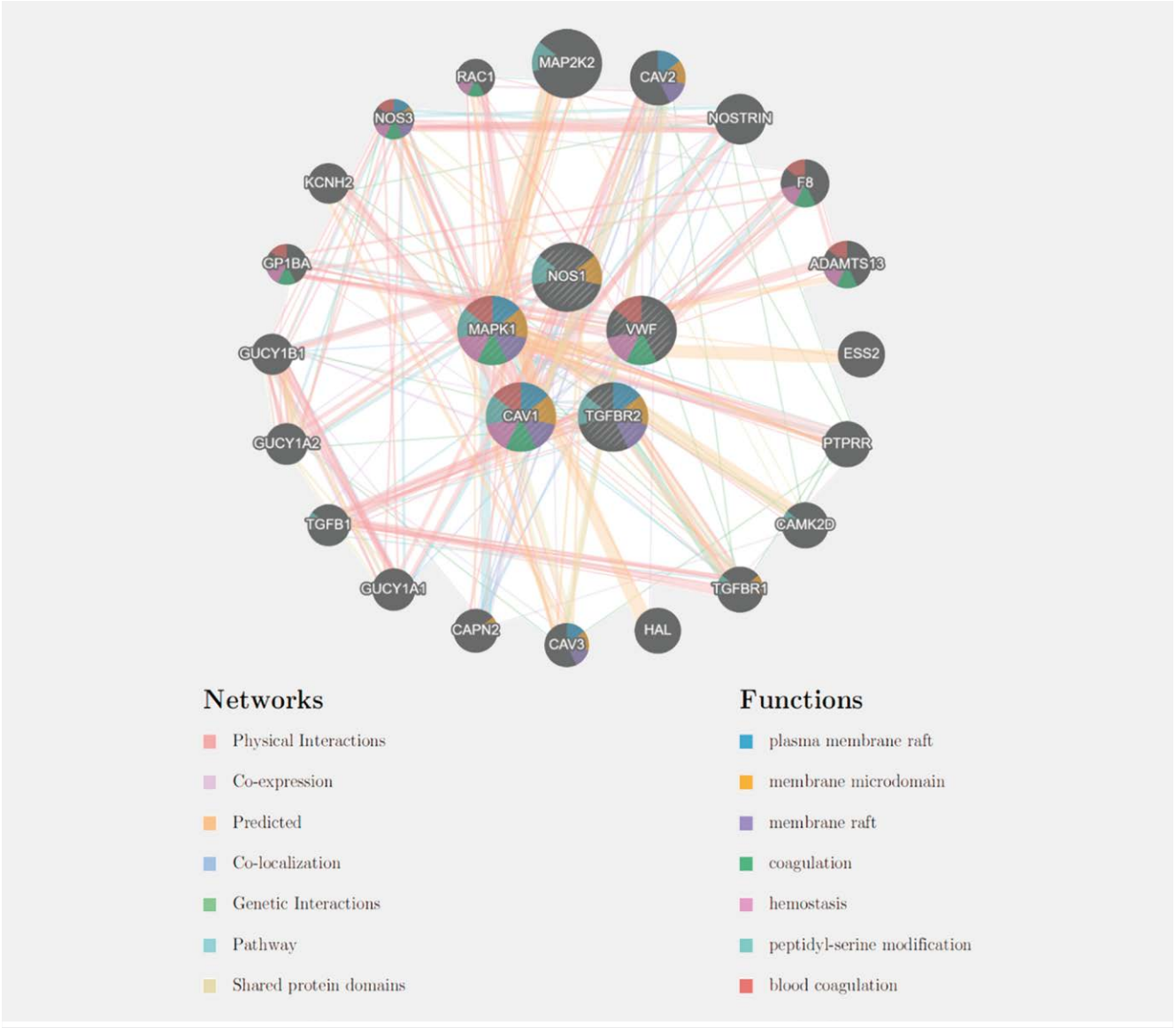

▶ **Fig. 4** Hub genes and their co-expression genes were analyzed via GeneMANIA.

VWF is a glycoprotein that plays a role in hemostasis. Thyroid hormone has been shown in vitro and in vivo to inhibit VWF synthesis in endothelial cells by controlling VWF gene transcription [26]. VWF expression is increased in hyperthyroid injury and vascular endothelial cells, and VWF knockdown inhibits thyroid carcinoma development by inhibiting cell proliferation, migration, and invasion [27]. VWF is an oncogene that plays a role in the occurrence and progression of thyroid carcinoma, but the expression of VWF in thyroid adenoma is low in our data set, requiring further confirmation.

The protein encoded by TGFBR2 represents the transmembrane protein that contains one protein kinase domain responsible for the phosphorylation of proteins entering the nucleus while regulating gene transcription during cell growth, tumor occurrence, cell cycle arrest, immunosuppression, and wound healing. In a genetic study, TGFBR2 was detected in thyroid-associated eye disease [28]. Peres et al. studied how single nucleotide polymorphisms (SNPs) affected the risk of cancer and observed that TGFBR2 was downregulated in both papillary thyroid cancer (PTC) and FTA histological types [29]. In our study, TGFBR2 was decreased in both thyroid and parathyroid adenomas, corresponding to the above findings. Recent studies have demonstrated that the effect of TGFBR2 on the occurrence of autoimmune thyroid disease is determined by its concentration and the signaling pathway affected by it, which makes it an effective marker for diagnosing and predicting the prognosis of thyroid autoimmune evolution [30]. TGFBR2 has a critical effect on the proliferation and autoimmune function of thyroid cells, as well as the parathyroid gland.

Previous research has suggested that CAV1 downregulation may aid in the proliferation and function of adenomatous PT cells. CAV1 is a powerful negative regulator of several mitogenic signaling pathways. CAV1 downregulation in parathyroid tissue may contrib-

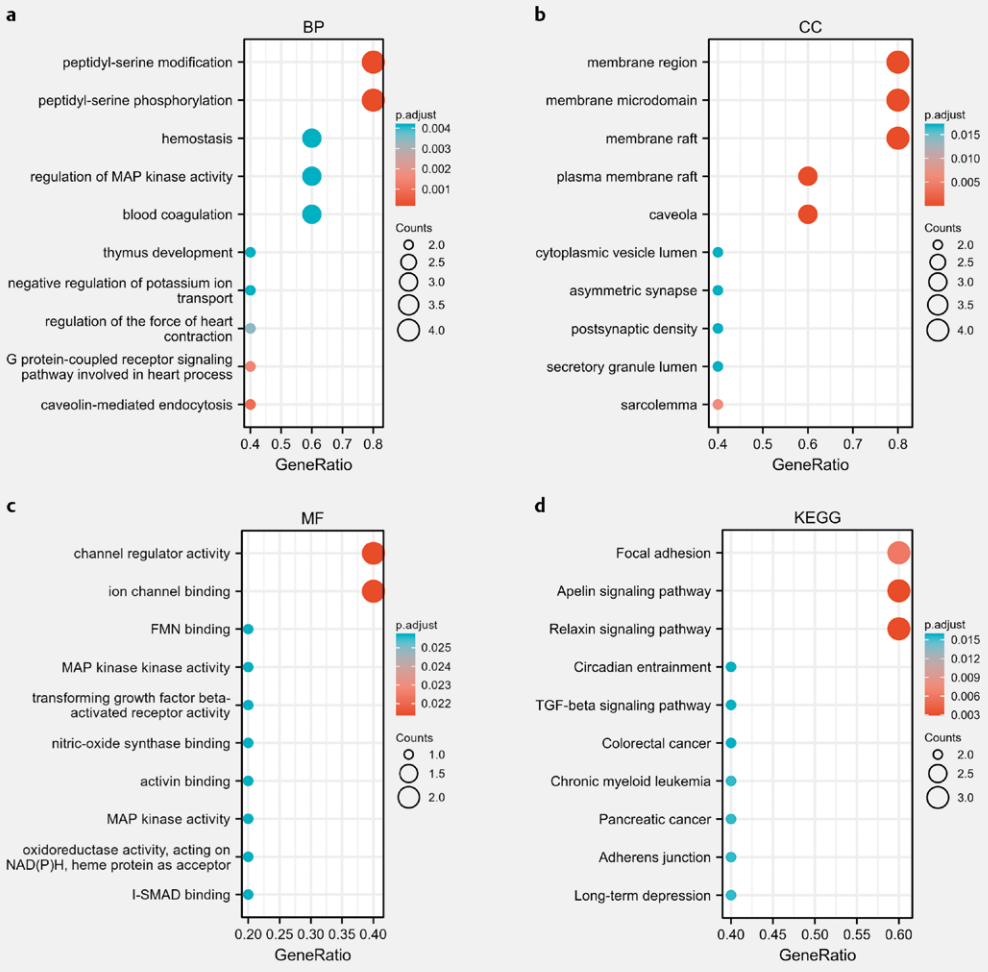

▶ **Fig. 5** Enrichment analysis of five hub genes (**a**, **b**, **c**, **d**) Bubble diagram: The circle size represents the number of enriched genes, and the color represents the p-value corresponding to the enrichment results.

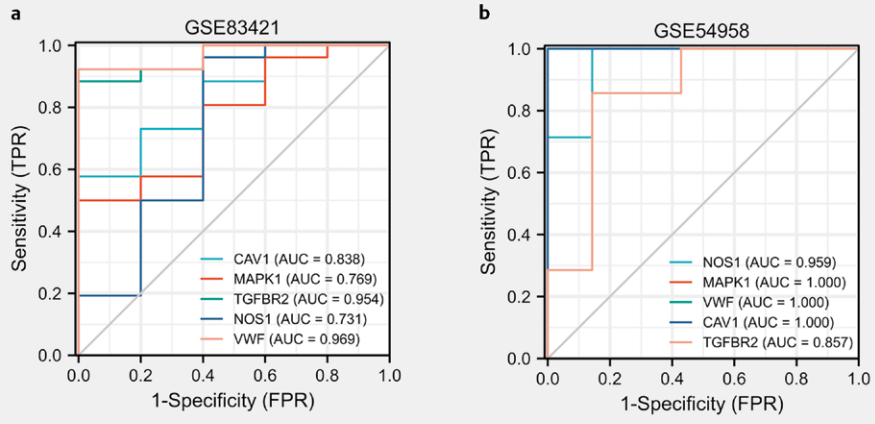

▶ **Fig. 6** Diagnostic ROC curves of 5 co-expressed hub genes between GSE83421 and GSE54958.

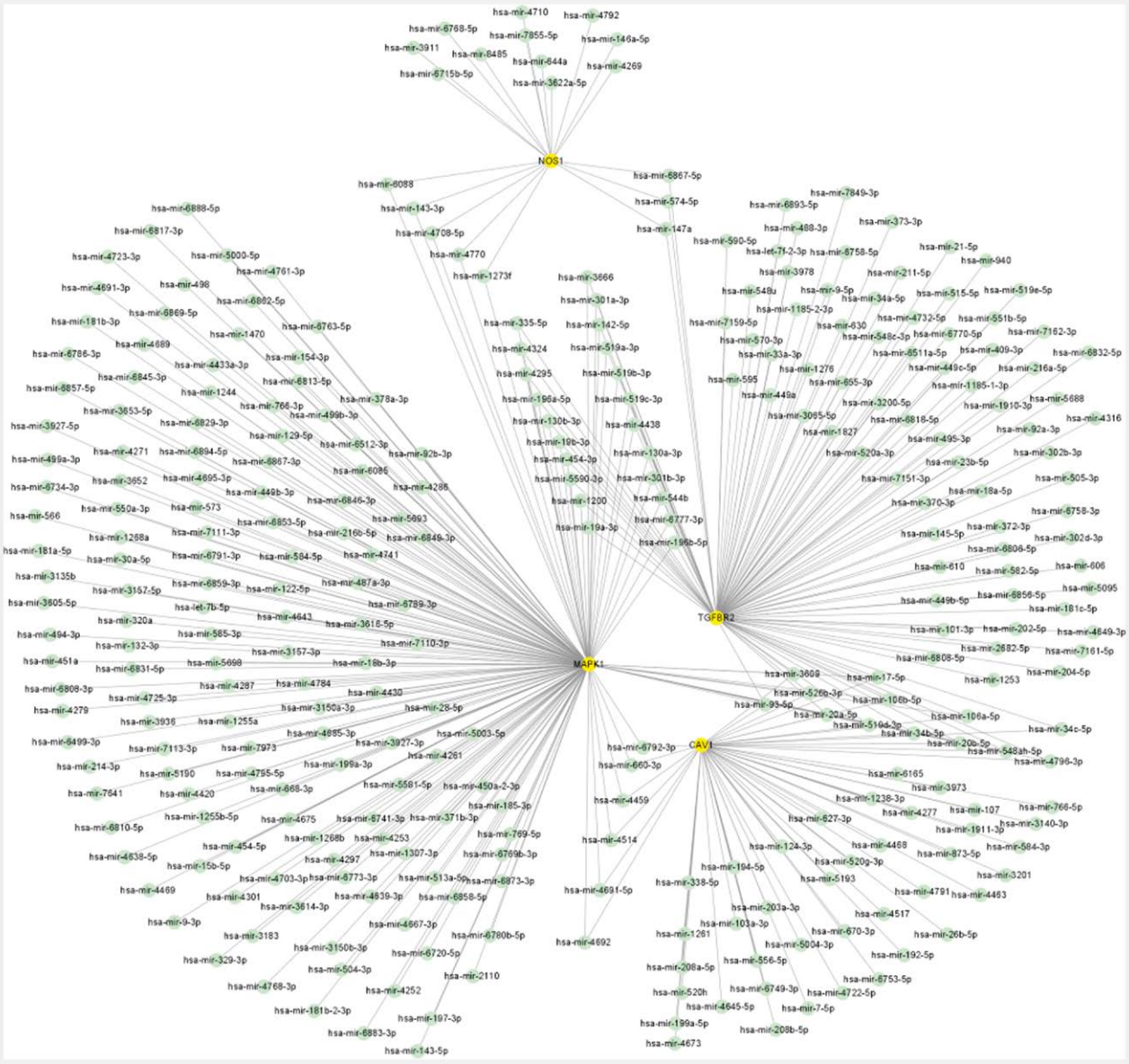

▶ **Fig. 7** MRNA-miRNA regulatory network of 5 co-expressed hub genes.

▶ **Table 2** The effective drugs targeted hub genes.

Gene names	Interaction type	Drug names	Interaction score
VWF	inhibitor	Caplacizumab	13.25
MAPK1	inhibitor	Ravoxertinib	0.58
NOS1	inhibitor	Ketamine	–
TGFBR2	inhibitor	Fostamatinib	–

ute to increased activity of cyclin D1, which is involved in the pathogenesis of a greater proportion of PAs [31]. CAV1 expression was found to be upregulated in all three differentiated thyroid cancer cell lines studied by Jay et al. [32]. However, no research on adenoma has been found. The results of the data set analysis in this study revealed that CAV1 was highly expressed in PA and decreased in FTA.

MAPK1 participates in a variety of processes, such as cell proliferation, differentiation, transcriptional regulation, and development as an integration point for a variety of biochemical signals. Our analysis is somewhat similar to that of Wang et al., who examined the thyroid cancer dataset (GSE27155) containing four healthy thyroid, 14 FTC, and 10 FTA tissues and detected some important pathways and genes [33]. One study on PTC reported that the over-

expression of ERBB4 or MAPK1 ameliorated the activity of mir-326 in the growth, invasion, and migration of PTC cells [34]. Another study also suggested that the inhibitory effect of MAPK1 was critical in thyroid cancer [35]. These results are consistent with the decreased expression of MAPK1 in thyroid adenoma in this study, which further strengthens our attention to MAPK1.

Finally, four potential therapeutic drugs (Caplacizumab, Ravoxertinib, Ketamine, and Fostamatinib) were identified by searching the DGIDB drug database, which may be a breakthrough in the treatment of PA and FTA. Among which Caplacizumab, a VWF-targeting drug, blocks the interaction between platelets and super giant von Willebrand factor multimer, thus, decreasing the platelet consumption and adhesion mediated by VWF. However, there are still no reports on the effect of this drug on adenoma. As a targeted inhibitor of MAPK1 and ERK kinase [36, 37]. Ravoxertinib has a critical effect on the inhibition of cancer cell growth. Studies have demonstrated that Ravoxertinib can reverse the nuclear-to-cytoplasmic localization defect of Nfatct in lymphatic dilatation and chylous accumulation during the development of the basement membrane, eventually improving the survival of endothelial KRAS-mutant newborn mice [38]. However, the relationship of this drug with adenomatous changes has not been reported and needs further investigation.

Our study has certain limitations. First, the relevant literature was downloaded from the GEO database as a representative dataset, and because of the low sample size, we may not adequately represent the results obtained from the other dataset. Moreover, we could not further validate our bioinformatics analysis experimentally. Therefore, further studies are needed to explore the common pathogenesis of PA and FTA.

In summary, we have observed five important hub genes common to PA and FTA, which had good diagnostic values. These genes are crucial to cell proliferation and tumor suppression, which also indicates that adenoma and cancer may be somewhat related. Our results provide some novel and common pathogenic genes, which may represent a breakthrough in the diagnosis and treatment of parathyroid adenoma and thyroid tumors. However, the exact co-pathogenesis of these two diseases still needs further study.

Acknowledgements

We thank all the public databases and websites used in this paper: The GEO database, The GO database, The KEGG Database, The STRING database, the GeneMANIA database, The NetworkAnalyst3,0 database, The online database ENCORI and The DSigDB database.

Funding Information

Natural Science Foundation of Fujian Province — http://dx.doi.org/10.13039/501100003392; 2021J011330; Natural Science Foundation of Xiamen City — http://dx.doi.org/10.13039/100016808; 3502Z20194016

Conflict of Interest

The authors declare that they have no conflict of interest.

References

[1] Shi YH, Dixit J, Koh D et al. Functional and genetic studies of isolated cells from parathyroid tumors reveal the complex pathogenesis of parathyroid neoplasia. Proc Natl Acad Sci U S A 2014; 111: 3092–3097

[2] Ishii H, Mihai R, Watkinson JC et al. Systematic review of cure and recurrence rates following minimally invasive parathyroidectomy. BJS Open 2018; 2: 364–370

[3] Sala TD, Muresan S, Roman R et al. Hypercalcaemic crisis due to primary hyperparathyroidism: report of two cases. J Crit Care Med (Targu Mures) 2019; 5: 34–39

[4] Theurer SSU, Lorenz K, Dralle H et al. Ektopes Gewebe der Schilddrüse und der Nebenschilddrüsen Ectopic tissue of the thyroid gland and the parathyroid glands. Pathologe 2018; 39: 379–389

[5] Rodrigo JP, Hernandez-Prera JC, Randolph GW et al. Parathyroid cancer: an update. Cancer Treat Rev 2020; 86: 102012

[6] Verdelli C, Morotti A, Tavanti GS et al. The core stem genes SOX2, POU5F1/OCT4, and NANOG are expressed in human parathyroid tumors and modulated by MEN1, YAP1, and beta-catenin pathways activation. Biomedicines 2021; 9: 637

[7] Papanikolaou A, Katsamakas M, Boudina M, Pamporaki C et al. Intrathyroidal parathyroid adenoma mimicking thyroid cancer. Endocrine Journal 2020; 67: 639–643

[8] Saljo K, Thornell A, Jin C et al. Characterization of glycosphingolipids in the human parathyroid and thyroid glands. Int J Mol Sci 2021; 22: 7044

[9] Erickson LA, Mete O, Juhlin CC et al. Overview of the 2022 WHO classification of parathyroid tumors. Endocr Pathol 2022; 33: 64–89

[10] Michael P, Bannon MD, Van Heerden MB et al. The relationship between primary hyperparathyroidism and diabetes mellitus. Ann Surg 1988; 207: 430–433

[11] Paloyan Walker RKE, Gopalsami C, Bassali J et al. Hyperparathyroidism associated with a chronic hypothyroid state. Laryngoscope 1997; 107: 903–909

[12] Yavropoulou MP, Poulios C, Michalopoulos N et al. A role for circular non-coding RNAs in the pathogenesis of sporadic parathyroid adenomas and the impact of gender-specific epigenetic regulation. Cells 2018; 8: 15

[13] Verdelli C, Forno I, Vaira V et al. Epigenetic alterations in human parathyroid tumors. Endocrine 2015; 49: 324–332

[14] Vaira V, Elli F, Forno I et al. The microRNA cluster C19MC is deregulated in parathyroid tumours. J Mol Endocrinol 2012; 49: 115–124

[15] Hu Y, Zhang X, Cui M et al. Circular RNA profile of parathyroid neoplasms: analysis of co-expression networks of circular RNAs and mRNAs. RNA Biol 2019; 16: 1228–1236

[16] Li Q, Li Y, Sun X et al. Genomic analysis of abnormal DNAM methylation in parathyroid tumors. Int J Endocrinol 2022; 4995196:

[17] The Gene Ontology C The gene ontology resource: 20 years and still GOing strong. Nucleic Acids Res 2019; 47: D330–D338

[18] Kanehisa M, Furumichi M, Sato Y et al. KEGG: integrating viruses and cellular organisms. Nucleic Acids Res 2021; 49: D545–D551

[19] Szklarczyk D, Gable AL, Lyon D et al. STRING v11: protein-protein association networks with increased coverage, supporting functional discovery in genome-wide experimental datasets. Nucleic Acids Res 2019; 47: D607–D613

[20] Otasek D, Morris JH, Boucas J et al. Cytoscape automation: empowering workflow-based network analysis. Genome Biol 2019; 20: 185

[21] Zhou G, Soufan O, Ewald J et al. NetworkAnalyst 3.0: a visual analytics platform for comprehensive gene expression profiling and meta-analysis. Nucleic Acids Res 2019; 47: W234–W241

[22] Freshour SL, Kiwala S, Cotto KC et al. Integration of the drug-gene interaction database (DGIdb 4.0) with open crowdsource efforts. Nucleic Acids Res 2021; 49: D1144–D1151

[23] Fukumura D, Kashiwagi S, Jain RK. The role of nitric oxide in tumour progression. Nat Rev Cancer 2006; 6: 521–534

[24] Li X, Zou Z, Tang J et al. NOS1 upregulates ABCG2 expression contributing to DDP chemoresistance in ovarian cancer cells. Oncol Lett 2019; 17: 1595–1602

[25] Wang Q, Ye S, Chen X et al. Mitochondrial NOS1 suppresses apoptosis in colon cancer cells through increasing SIRT3 activity. Biochem Biophys Res Commun 2019; 515: 517–523

[26] Brait M, Loyo M, Rosenbaum E et al. Correlation between BRAF mutation and promoter methylation of TIMP3, RARbeta2 and RASSF1A in thyroid cancer. Epigenetics 2012; 7: 710–719

[27] Kong QFLB, Wang B, Zhang XP et al. Association of von Willebrand factor (vWF) expression with lymph node metastasis and hemodynamics in papillary thyroid carcinoma. Eur Rev Med Pharmacol Sci 2020; 24: 2564–2571

[28] Mishra SMV, Kumar S, Ankita et al. Clinical management and therapeutic strategies for the thyroid-associated ophthalmopathy: current and future perspectives. Curr Eye Res 2020; 45: 1325–1341

[29] Peres KC, Teodoro L, Amaral LHP et al. Clinical utility of TGFB1 and its receptors (TGFBR1 and TGFBR2) in thyroid nodules: evaluation based on single nucleotide polymorphisms and mRNA analysis. Arch Endocrinol Metab 2021; 65: 172–184

[30] Kardalas E, Sakkas E, Ruchala M et al. The role of transforming growth factor beta in thyroid autoimmunity: current knowledge and future perspectives. Rev Endocr Metab Disord 2022; 23: 47

[31] Imam N, Alam A, Siddiqui MF et al. Identification of key regulators in parathyroid adenoma using an integrative gene network analysis. Bioinformation 2020; 16: 910–922

[32] Shankar J, Wiseman SM, Meng F et al. Coordinated expression of galectin-3 and caveolin-1 in thyroid cancer. J Pathol 2012; 228: 56–66

[33] Chai YJ, Chae H, Kim K et al. Comparative gene expression profiles in parathyroid adenoma and normal parathyroid tissue. J Clin Med 2019; 8: 297

[34] Nie FR, Li QX, Wei HF et al. miR-326 inhibits the progression of papillary thyroid carcinoma by targeting MAPK1 and ERBB4. Neoplasma 2020; 67: 604–613

[35] Chen H, Li Q, Yi R et al. CircRNA casein kinase 1 gamma 1 (circ-CSNK1G1) plays carcinogenic effects in thyroid cancer by acting as miR-149-5p sponge and relieving the suppression of miR-149-5p on mitogen-activated protein kinase 1 (MAPK1). J Clin Lab Anal 2022; 36: e24188

[36] Blake JF, Burkard M, Chan J et al. Discovery of (*S*)-1-(1-(4-Chloro-3-fluorophenyl)-2-hydroxyethyl)-4-(2-((1-methyl-1*H*-pyrazol-5-y l) amino)pyrimidin-4-yl)pyridin-2(1*H*)-one (GDC-0994), an extracellular signal-regulated kinase 1/2 (ERK1/2) inhibitor in early clinical development. J Med Chem 2016; 59: 5650–5660

[37] Zhu J, Wang J, Wang X et al. Prediction of drug efficacy from transcriptional profiles with deep learning. Nat Biotechnol 2021; 39: 1444–1452

[38] Janardhan HP, Dresser K, Hutchinson L et al. Pathological MAPK activation-mediated lymphatic basement membrane disruption causes lymphangiectasia that is treatable with ravoxertinib. JCI Insight 2022; 7: e153033